

LETTER

Directional biases and resource-dependence in dispersal generate spatial patterning in a consumer–producer model

Kurt E. Anderson,^{1*} Frank M. Hilker² and Roger M. Nisbet³

Abstract

Directional dispersal plays a large role in shaping ecological processes in diverse systems such as rivers, coastlines and vegetation communities. We describe an instability driven by directional dispersal in a spatially explicit consumer–producer model where spatial patterns emerge in the absence of external environmental variation. Dispersal of the consumer has both undirected and directed components that are functions of producer biomass. We demonstrate that directional dispersal is required for the instability, while undirected diffusive dispersal sets a lower bound to the spatial scale of emerging patterns. Furthermore, instability requires indirect feedbacks affecting consumer per capita dispersal rates, and not activator–inhibitor dynamics affecting production and mortality as is described in previous theory. This novel and less-restrictive mechanism for generating spatial patterns can arise over realistic parameter values, which we explore using an empirically inspired model and data on stream macroinvertebrates.

Keywords

Advection, consumer–resource interactions, dispersal, flow-induced instability, spatial dynamics, streams and rivers, Turing instability.

Ecology Letters (2012) 15: 209–217

INTRODUCTION

Directional dispersal shapes ecological processes in systems with flowing dispersal media. Environments such as streams and rivers (Waters 1972; Williams & Williams 1993), coastlines (Byers & Pringle 2006) and vegetation communities (Levine 2003) experience strong coupling among spatially separated sites because of the directional dispersal of individuals and/or transport of abiotic resources.

Streams and rivers are iconic examples of systems influenced by directional transport, and many of the conceptual foundations of stream ecology address the effects of transport by flow (Vannote *et al.* 1980; Townsend 1989; Newbold 1992). A variety of stream organisms drift in the water column (Elliott 1971; Palmer *et al.* 1996) and respond to the local environmental conditions through dispersal (Kohler 1985; Winterbottom *et al.* 1997; Diehl *et al.* 2000; Englund *et al.* 2001; Roll *et al.* 2005). Accordingly, consumer–resource interactions over small spatial and temporal scales may be more greatly influenced by immigration and emigration than by production and mortality (Fonseca & Hart 1996; Nisbet *et al.* 1997; Diehl *et al.* 2000; Englund *et al.* 2001; Englund & Hamback 2004; Roll *et al.* 2005). As a result, intergenerational food-web dynamics and responses of these to environmental variation may manifest strongly only over larger scales, making it difficult to ‘scale up’ the results of small scale experiments (Cooper *et al.* 1998; Englund *et al.* 2001; Woodward & Hildrew 2002). Indeed, there is still a large gap in our understanding of how spatial variation in population densities and food-web structure are linked to local dynamics and environ-

mental conditions in streams and rivers (Woodward & Hildrew 2002).

While directionally biased dispersal may obscure consumer–resource outcomes by spatially separating driver from effect, consumer–resource theory also suggests that spatial variation can be generated or exacerbated by demographic feedbacks working in concert with dispersal (Murray 2003; Malchow *et al.* 2008). A classic example is diffusive instability where ‘random’ dispersal can lead to non-equilibrium spatial variation in consumer and resource populations, even in the absence of environmental variation (Segel & Jackson 1972). For such patterns to occur, producers must positively affect their own and consumer densities, while consumers have the opposite effect. The consumer species must also diffuse much faster than the resource species. More recently, a second mechanism of dispersal-driven pattern formation has been investigated focusing on directional dispersal – advection – rather than diffusion (Rovinsky & Menzinger 1992; Malchow *et al.* 2008). Under these so-called ‘flow-induced instabilities’ (or FII’s), the restrictive conditions on movement differences are somewhat relaxed, but those on producer–consumer feedbacks are not. Spatial instabilities driven by advection have been invoked to explain spatial patterns in planktonic food chains (Malchow *et al.* 2008), juvenile mussel beds (van de Koppel *et al.* 2005), and vegetation communities (Sherratt 2005).

Flow-induced instabilities have obvious potential for shaping ecological dynamics in streams and other flowing environments, as organisms in these systems express wide variation in dispersal (e.g. Rader 1997). Feedbacks between consumers and resources often

¹Department of Biology, University of California, Riverside CA 92521, USA

²Department of Mathematical and Statistical Sciences, Centre for Mathematical Biology, University of Alberta, Edmonton AB T6G 2G1, Canada; and Centre for Mathematical Biology and Department of Mathematical Sciences, University of Bath, Bath BA2 7AY, UK

³Department of Ecology, Evolution, and Marine Biology, University of California, Santa Barbara CA 93106-9620, USA

*Correspondence: E-mail: kurt.anderson@ucr.edu

manifest at local scales as changes in per capita emigration rates rather than (or in addition to) changes in production and mortality rates. It may be possible for these feedbacks – mediated by directional dispersal – to structure non-equilibrium spatial patterns at larger spatial and temporal scales. Our ability to predict when these features might lead to spatial variation could be greatly enhanced by models of the basic processes – theory that is currently lacking.

Herein, we investigate spatial instability in consumer–resource models where consumer dispersal has both resource-dependence and a directional bias. Using a strategic model, we demonstrate that instability requires both of these features. We then extend our results to an empirically motivated model that describes dispersal using easily measured emigration and drift dispersal terms. The novel, less restrictive mechanism for generating spatial patterns we report has wide implications for ecological dynamics in systems with biased transport, which we explore using data on stream macroinvertebrates.

SPATIAL INSTABILITIES IN A REACTION–DIFFUSION–ADVECTION PRODUCER–CONSUMER MODEL

Previous theory shows that non-equilibrium spatial patterns can occur in consumer–resource models, when dispersal is ‘random’ or directionally biased. We begin by examining the contributions of these two dispersal types to instability when consumer–resource interactions alter consumer dispersal rates. We use a reaction–diffusion–advection (RDA) formalism, which has been used extensively in analyses of diffusive and flow-induced instabilities, allowing us to build on previous theory.

Consider a resource producer with biomass density $P(x, t)$ and a consumer with density $C(x, t)$ at stream location x and time t with dynamics described by

$$\begin{aligned} \frac{\partial P(x, t)}{\partial t} &= \underbrace{I_P}_{\text{production}} - \underbrace{f(P(x, t))C(x, t)}_{\text{losses to consumption}} \\ \frac{\partial C(x, t)}{\partial t} &= \underbrace{I_C}_{\text{recruitment}} - \underbrace{mC(x, t)}_{\text{mortality}} - \underbrace{\frac{\partial}{\partial x}[v(P(x, t))C(x, t)]}_{\text{advection}} \\ &+ \underbrace{\frac{\partial^2}{\partial x^2}[D(P(x, t))C(x, t)]}_{\text{diffusion}}. \end{aligned} \quad (1)$$

Streams and other advective systems are often ‘open’ systems (Palmer *et al.* 1996), where production can be driven by allochthonous nutrient supply or recruitment from egg banks laid by adults that reside outside the system. Thus, both species recruit at constant rates independent of local density in our model. Consumers reduce producer biomass through consumption, with functional response $f(P(x, t))$, where $\partial f(P)/\partial P > 0$, and die at a constant per capita rate m .

Producers are assumed immobile and consumers disperse using both diffusion and advection. Diffusion approximates stochastic displacement, such as by turbulence or in active response to multiple unmeasured factors, that lacks a net directional bias. Advection describes directional components of dispersal in the downstream direction. Consumers respond to low producer biomass through increased advection and diffusion rates, i.e. $\partial v(P)/\partial P < 0$ and $\partial D(P)/\partial P < 0$.

Analysis of the spatial instability

Numerical simulations of eq. (1) reveal the presence of spatial instabilities manifesting as travelling waves moving in the direction of advection (Fig. 1). These waves represent consumers ‘chasing’ producers through downstream advection, depleting the trailing edge of producer waves via consumption. Consumers build up on the trailing edge of producer waves as a result of density-dependent dispersal: consumers rapidly emigrate from areas of low producer biomass and stay in high biomass ones. The aggregation of consumers in turn opens consumer-free space where producers are replenished. Extensive simulations suggest that these qualitative spatial patterns are consistent regardless of specific functional forms used for consumption and dispersal as long as they are constrained as outlined above. However, whether these patterns form in the first place depends greatly on parameter values.

Effects of parameters on instability are elucidated using linear stability analysis; that is, by examining whether small deviations from a spatially uniform steady state (P^* , C^*) grow or decay (Murray 2003). Deviations $P(x, t) = P^* + \tilde{p}(x, t)$ and $C(x, t) = C^* + \tilde{c}(x, t)$ that grow indicate instability and the presence of non-equilibrium spatial patterns. Progress is facilitated by Fourier analysis, which, when applied to the spatial dimension x , represents spatial variation in $\tilde{p}(x, t)$ and $\tilde{c}(x, t)$ as the integral of sinusoids with different spatial frequencies k ,

$$\begin{aligned} \tilde{p}(k, t) &= \int_{-\infty}^{\infty} \tilde{p}(x, t) e^{-ikx} dx \quad \text{and} \\ \tilde{c}(k, t) &= \int_{-\infty}^{\infty} \tilde{c}(x, t) e^{-ikx} dx. \end{aligned} \quad (2)$$

The spatial frequency k (often referred to as the wavenumber) is inversely proportional to the spatial wavelength, or spatial scale, over

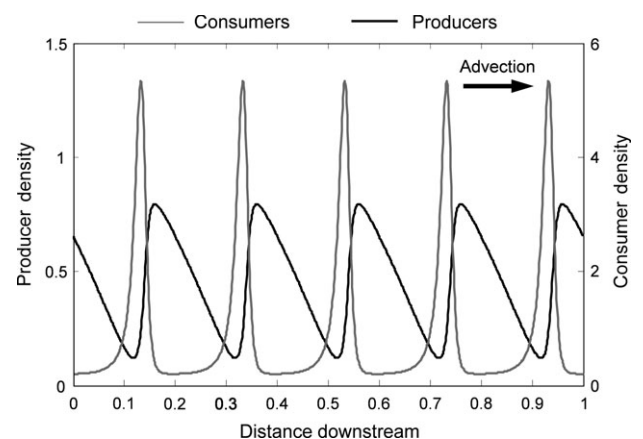


Figure 1 An example of spatial instabilities that arise in the RDA producer–consumer model in eq. (1) generated using numerical simulations with periodic boundary conditions. Producer density $P(x, t)$ and consumer density $C(x, t)$ were calculated using the finite element method and PARDISO direct linear solver in COMSOL Multiphysics™. The spatial waves shown travel in the direction of downstream advection at 0.135 units distance/unit time. Functions are $f(P) = \sigma P$, $v(P) = v_0 \exp[-v_r P]$, $D(P) = d_0 \exp[-d_r P]$; parameter values are $I_P = 1$; $\sigma = 3.1$; $I_C = 0.1$; $m = 0.1$; $v_0 = 0.2$; $v_r = 1.8$; $d_0 = 0.0005$; $d_r = 0$.

which the sinusoidal component varies. Each spatial frequency contributes to the overall pattern of spatial variation in the state variables. In real ecological systems, populations will always deviate from uniform steady-states with decidedly non-uniform spatial distributions. Yet those spatial distributions can always be broken down into components with different spatial frequencies k . Of the range of spatial frequencies present in producer or consumer deviations, those frequencies that are unstable will grow, while those that are stable will decay.

After re-casting eq. (1) into small deviations (ignoring small non-linear terms) and applying Fourier transforms from eq. (2), the system takes the form of a pair of linear ordinary differential equations. Rewritten in vector-matrix form for convenience,

$$\frac{\partial \tilde{\mathbf{n}}}{\partial t} = \mathbf{J}\tilde{\mathbf{n}}, \text{ where } \tilde{\mathbf{n}} = \begin{bmatrix} \tilde{p} \\ \tilde{c} \end{bmatrix} \text{ and}$$

$$\mathbf{J} = \begin{bmatrix} -f'(P^*)C^* & -f(P^*) \\ -v'(P^*)C^*ik - D'(P^*)C^*k^2 & -m - v(P^*)ik - D(P^*)k^2 \end{bmatrix}. \quad (3)$$

Equation (3) reveals important generalisations about instability in the RDA model, which we now explore.

The first major generalisation is that instability depends on the spatial frequencies k (see Online Supplement S1 in Supporting Information). The RDA approximation in eq. (3) has eigenvalues $\lambda_{1,2} = \rho_{1,2} + i\omega_{1,2}$ where ρ and ω are the real and imaginary parts of λ , respectively, and $i = \sqrt{-1}$. The system becomes unstable if the real part ρ of any eigenvalue becomes greater than zero (Fig. 2), and the instability involves travelling waves when ω is non-zero. Both ρ and ω are always functions of k , and ω is non-zero for $k > 0$.

The unstable components grow and lead to persistent non-equilibrium spatial patterns (as in Fig. 1). These take the form of travelling waves with peaks separated by a distance of approximately $\frac{2\pi}{k_{max}}$ that proceed downstream at speed $\frac{\omega}{k_{max}}$ where k_{max} is the frequency of the least stable component (the largest positive ρ).

Non-linear terms ignored in eq. (3) do eventually become large, causing the waves to cease growing in amplitude and become less sinusoidal in shape (Fig. 1, Online Supplement S2).

A second major generalisation is that advection is necessary for instability. The RDA with diffusion and no advection (i.e. $D(P^*) > 0$, $D'(P^*) > 0$, $v(P^*) = v'(P^*) = 0$) is stable under all parameter combinations (Murray 2003). With advection, and in the absence of diffusion (i.e. $D(P^*) = D'(P^*) = 0$), the relationship between k and ρ_1 mirrors that of many systems exhibiting flow-induced instabilities (Malchow *et al.* 2008): ρ_1 becomes positive at some critical wave-number k_v and continues to rise monotonically for all $k > k_v$ under unstable parameter combinations (Fig. 2). Spatially uniform deviations ($k = 0$) are always stable (Online Supplement S1). Thus, advection causes the system to become unstable over all spatial frequencies higher than k_v , meaning that the non-equilibrium patterns generally occur with small spatial wavelengths.

When advection is combined with diffusion, the RDA model can still become unstable at sufficiently large k_v (Fig. 2). However, diffusion stabilizes spatial frequencies exceeding a second critical value k_d yielding a k_{max} that occurs at the peak of the resulting unimodal dispersion relation, where $k_v < k_{max} < k_d$. This is because aggregations are typically smoothed by diffusion as individuals move from areas of high to low density. Advection does not offer such smoothing properties and thus provides no mechanism to dampen spatial variation.

Our final generalisation is that spatial instabilities occur in our producer–consumer system despite its lacking ‘activator–inhibitor’ dynamics, a key requirement for traditional diffusive and previously examined differential flow-induced instabilities to form. Ignoring terms related to dispersal (i.e. operating on ik or k^2 terms), the Jacobian matrix for a typical activator–inhibitor system has signs

$$\mathbf{J} = \begin{pmatrix} + & - \\ + & - \end{pmatrix}. \quad (4)$$

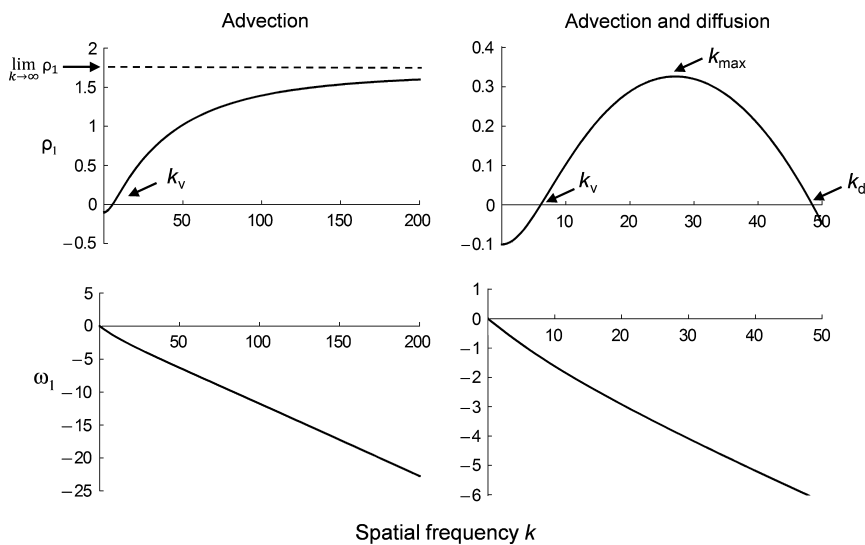


Figure 2 Relationship between instability and spatial frequency k (radians/length) for eq. (3). The real part of the dominant eigenvalue ρ_1 gives the rate at which deviations from uniform steady state initially grow or decay. In the advection only case, values of ρ_1 are unstable for spatial frequencies larger than k_v . In the advection and diffusion case, spatial frequencies are unstable between $k_v < k < k_d$ and the fastest growing spatial frequency is given by k_{max} . Negative values of ω_1 (radians/time) indicate that spatial patterns manifest as travelling waves. Functional forms and parameter values are as in Fig. 1 with the exception that $d_0 = 0$ in the advection only case.

The positive signs in the first column reflect producers having a positive or ‘activating’ effect on their own and their consumer’s densities through births. The negative signs reflect consumers having likewise negative or ‘inhibiting’ effects through consumption and death. In contrast, the signs under the same non-spatial conditions ($v(P^*) = v'(P^*) = D(P^*) = D'(P^*) = 0$) in our system are

$$\mathbf{J} = \begin{pmatrix} - & - \\ 0 & - \end{pmatrix}. \tag{5}$$

Consumers still have inhibitory effects, but producers no longer have activating effects in the absence of dispersal. Consumer ‘activation’ by producers reappears when producer-dependence in consumer dispersal is added, indicating that this feedback affecting dispersal rates is required, but not sufficient, for the instability to form (Supplement S1). We now proceed to explore how producer-dependent and downstream-biased dispersal drive instability through parameter studies.

Parameter studies

We limit our analyses to cases with a linear functional response for consumer grazing,

$$f(P) = \sigma P \tag{6}$$

where σ is the per capita consumption rate. However, we observe qualitatively similar dynamics with other functional responses. We non-dimensionalise the equations by scaling time relative to the aver-

age consumer lifetime m^{-1} , and scaling space relative to the average distance a consumer in the steady state population disperses downstream via advection during its lifetime, i.e. $v(P^*)/m$. Consumer and producer densities are scaled relative to their uniform space steady state values. Thus, if hats denote scaled (dimensionless) quantities, we define

$$\hat{t} = mt, \quad \hat{x} = mx/v, \quad \hat{k} = vk/m, \quad \hat{p} = p/P^*, \quad \hat{c} = c/C^*. \tag{7}$$

We then define the dimensionless parameter groups

$$\hat{\sigma} = \frac{\sigma C^*}{m}, \quad \beta = -\frac{P^* v'(P^*)}{v(P^*)}, \quad \hat{D} = \frac{mD(P^*)}{[v(P^*)]^2}, \quad \delta = -\frac{mP^* D'(P^*)}{[v(P^*)]^2}. \tag{8}$$

The dimensionless form of the Jacobian (eq. 3) is then

$$\hat{\mathbf{J}} = \begin{bmatrix} -\hat{\sigma} & -\hat{\sigma} \\ \beta i \hat{k} + \delta \hat{k}^2 & -1 - i \hat{k} - \hat{D} \hat{k}^2 \end{bmatrix}, \tag{9}$$

and the linearised dynamics are controlled by four dimensionless parameters: the scaled strength of consumption $\hat{\sigma}$, the strength of advection sensitivity to producer variation β , a parameter \hat{D} that represents the relative contributions of diffusion and advection to an organism’s average lifetime displacement, and a measure of the strength of diffusion sensitivity to producer variation, δ .

The effects of the controlling parameters on the onset of instability as well as the spatial scale over which the instability manifests are shown in Fig. 3. Both advection sensitivity β and scaled consumption $\hat{\sigma}$ must be sufficiently large in order for instability to form. In the simple case of dispersal by advection only ($\hat{D} = \delta = 0$),

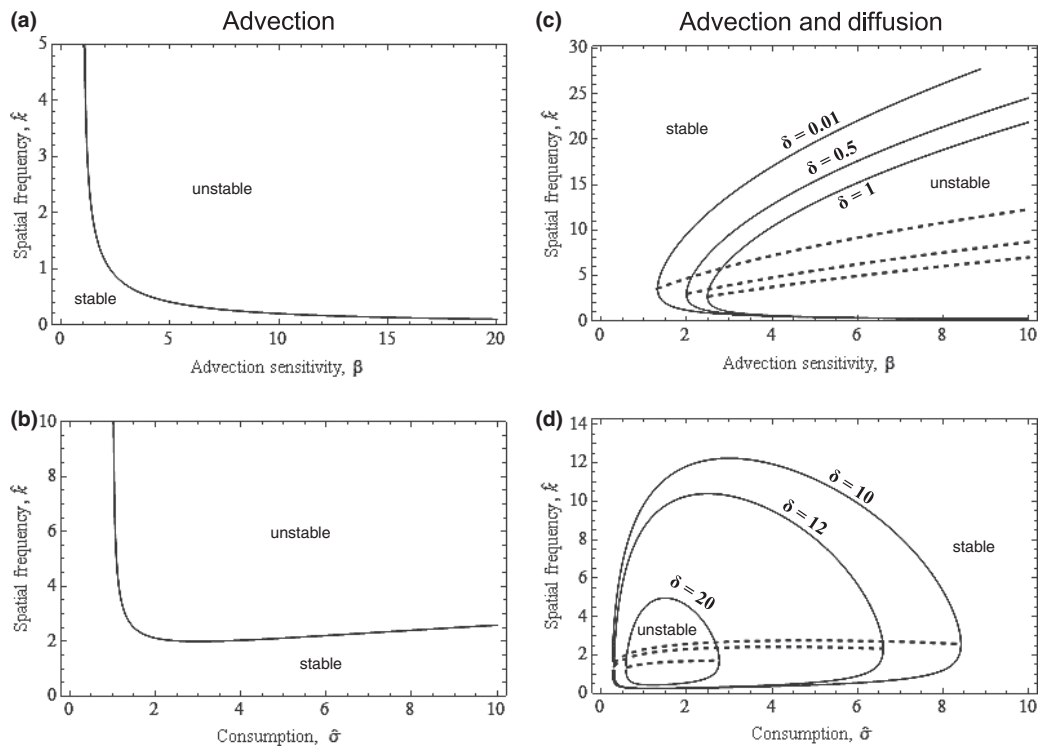


Figure 3 Effects of parameters on system stability in the RDA model eq. (9). For a given set of parameter values, unstable frequencies are those bounded by critical frequencies \hat{k}_c . The critical spatial frequency \hat{k}_c in (a) and (b) is k_c . In (c) and (d), the critical spatial frequency \hat{k}_c is equal to k_c in the lower solid branch and k_d in the upper solid branch. Both are represented by black solid lines (—). The fastest growing spatial frequency \hat{k}_{max} is represented by grey dashed lines (- - -). Parameters are (a) $\hat{\sigma} = 1, \hat{D} = 0, \delta = 0$; (b) $\beta = 10, \hat{D} = 0, \delta = 0$; (c) $\hat{\sigma} = 1, \hat{D} = 0.01$; (d) $\beta = 10, \hat{D} = 0.01$.

$$\lim_{k \rightarrow \infty} \rho_1(k) = \frac{1}{2} (\text{abs}(\sigma - 1 + 2\beta\sigma) - \sigma - 1) \quad \text{and} \quad \hat{k}_v = \frac{\hat{\sigma} + 1}{\sqrt{\hat{\sigma}\beta^2 + \hat{\sigma}\beta - \beta - 1}}, \quad (10)$$

and hence instability occurs when $\hat{\sigma}\beta > 1$ with $\lim_{k \rightarrow \infty} \rho_1(k) = \hat{\sigma}\beta - 1$ (Fig. 3a,b). A positive advection sensitivity β leads to consumers leaving areas of low producer density at higher per-capita rates than areas of higher density. The instability arises as downstream consumers slow their advection after encountering high producer patches while upstream consumers simultaneously move quickly through areas of low producer biomass. As β increases, consumers become more sensitive to spatial variation in producer biomass, destabilising lower frequencies (i.e. longer spatial wavelengths) of perturbation despite weaker spatial producer gradients at these frequencies (Fig. 3a). Increasing consumption $\hat{\sigma}$, when low, promotes instabilities through maintenance of variation in producer biomass. However, once consumption becomes much stronger, further strengthening tends to destroy producer variation and increases system stability, especially in smaller spatial frequencies (Fig. 3b).

Diffusion, via both \hat{D} and its sensitivity to producers δ , increases the stability of the system (Fig. 3c,d, results for the former are not shown). As the contribution of diffusion increases, the sensitivity of the advection contribution required to destabilise the system increases as well (Fig. 3c). While in the unstable range of β , the highest unstable spatial frequency \hat{k}_d and the maximum unstable frequency \hat{k}_{max} both reduce with increasing contributions of diffusion. The lowest unstable frequency \hat{k}_v set by advection remains largely unaffected (Fig. 3c).

Diffusion also restricts the range of k where consumption destabilizes the system (Fig. 3d). Because consumption $\hat{\sigma}$ destroys producer variation when the wavelengths of this variation are very large or very small – the same scales that are typically smoothed over by diffusion – the instability only emerges over intermediate values of $\hat{\sigma}$ when diffusion is present. As above, diffusion strongly reduces the values of \hat{k}_d and \hat{k}_{max} but not \hat{k}_v over most values of consumption (Fig. 3d). These results reinforce our earlier qualitative generalisations that it is the advection and producer-dependent dispersal, and not the diffusion or activator–inhibitor dynamics, which leads to instability in the RDA model.

INSTABILITIES IN A MODEL OF EMIGRATION AND DRIFT

Our analysis of the RDA model reveals the roles played by advection, and by producer-dependence in advection rates, in establishing the spatial instability. We also demonstrated that diffusion, with and without producer-dependence, enhances stability. However, organisms in streams, rivers and other systems with directional dispersal do not necessarily exhibit such easily identifiable advection and diffusion phases of dispersal. Instead, individuals often appear to emigrate from locations one or more times during a life cycle and drift in the water column before resettling in a new location (see references in Palmer *et al.* 1996; Diehl *et al.* 2008). We now extend our results from the RDA model to an empirically motivated model that includes specific emigration and drift dispersal terms.

Our model is a generalisation of a stream consumer–producer system analyzed by (Anderson *et al.* 2008) that uses an *integro-differential equation* (IDE) for consumer dynamics,

$$\begin{aligned} \frac{\partial P(x,t)}{\partial t} &= \underbrace{I_p}_{\text{production}} - \underbrace{f(P(x,t))C(x,t)}_{\text{losses to consumption}} \\ \frac{\partial C(x,t)}{\partial t} &= \underbrace{I_C}_{\text{recruitment}} - \underbrace{mC(x,t)}_{\text{mortality}} - \underbrace{E(P(x,t))C(x,t)}_{\text{emigration}} \\ &+ \underbrace{\int_{-\infty}^{\infty} E(P(y,t))C(y,t)b(x-y) dy}_{\text{immigration}} \end{aligned} \quad (11)$$

Production, recruitment, consumption and mortality terms are defined as for eq. (1). Instead of advection and diffusion terms, eq. (11) assumes organisms emigrate from their current location at a per capita rate $E(P(x,t))$ that declines with increasing producer biomass, $\frac{\partial E}{\partial P} < 0$, and resettle according to the integral immigration term. We describe the resettlement process in the immigration term using the dispersal function $b(x,y)$ where $b(x-y)$ is the proportion of individuals emigrating from location y that settle instantaneously in the interval $(x, x + dx)$.

We restrict our choice of dispersal functions to probability distributions that are exponentially bounded in the tails, which includes many standard probability distributions (e.g. exponential and Gaussian) but excludes ‘fat-tailed’ distributions. We define L_D as the mean distance travelled per emigration event and M_2 as the second moment,

$$L_D = \int_{-\infty}^{\infty} ub(u)du, \quad M_2 = \int_{-\infty}^{\infty} u^2 b(u)du, \quad \text{and} \quad \int_{-\infty}^{\infty} b(u)du = 1. \quad (12)$$

Dispersal distributions for macroinvertebrates in streams and rivers have been observed possessing downstream skews (i.e. $L_D > 0$) (e.g. Elliott 1971; Englund & Hamback 2004).

To analyze our empirically motivated IDE model, we follow steps similar to those outlined for the RDA model to get from eq. (1) to eq. (9), with consumption also defined by eq. (6). We define $\tilde{b}(k)$ as the Fourier transform of the dispersal function $b(x,y)$, which we can approximate for small values of k without specifying the form of the kernel itself. Taking the Taylor expansion of $\tilde{b}(k)|_{k=0}$ and dropping terms $O(k)^3$ and higher,

$$\begin{aligned} \tilde{b}(k) &= \int_{-\infty}^{\infty} b(y)e^{-iky} dy \approx \int_{-\infty}^{\infty} b(y)(1 - iky - \frac{1}{2}k^2y^2)dy \\ &= 1 - ikL_D - \frac{1}{2}k^2M_2 \end{aligned} \quad (13)$$

where $L_D = \int_{-\infty}^{\infty} yb(y)dy$ and $M_2 = \int_{-\infty}^{\infty} y^2b(y)dy$.

After linearisation and Fourier transforming the spatial dimension, we define two forms of the IDE: a ‘generalized’ form that does not specify the form of consumer emigration, and a ‘specified’ form that represents consumer emigration explicitly. The generalised emigration IDE, after the re-parameterisation

$$\begin{aligned} \hat{t} &= mt, \quad \hat{x} = x/L_D, \quad \hat{k} = kL_D, \quad \hat{p} = p/P^*, \quad \hat{c} = c/C^*, \\ \varepsilon &= \frac{E(P^*)}{m}, \quad \varepsilon' = \frac{E'(P^*)P^*}{m}, \quad \hat{\sigma} = \frac{\sigma C^*}{m}, \end{aligned} \quad (14)$$

has Jacobian

$$J = \begin{bmatrix} -\hat{\sigma} & -\hat{\sigma} \\ \varepsilon'(i\hat{k} + \hat{k}^2) & -1 - \varepsilon(i\hat{k} + \hat{k}^2) \end{bmatrix}. \quad (15)$$

The specified emigration IDE includes the following representation of consumer emigration,

$$E(P) = e_0 \exp\{-\alpha P\} \quad (16)$$

where e_0 is the baseline consumer per-capita emigration rate and α is the sensitivity of emigration to producer biomass. We rescale by setting

$$\begin{aligned} \hat{t} &= mt, & \hat{x} &= x/L_D, & \hat{k} &= kL_D, & \hat{p} &= p/P^*, & \hat{c} &= c/C^*, \\ \hat{e}_0 &= \frac{e_0}{m}, & \hat{\alpha} &= \alpha P^*, & \hat{\sigma} &= \frac{\sigma C^*}{m}, \end{aligned} \quad (17)$$

which yields

$$J = \begin{bmatrix} -\hat{\sigma} & -\hat{\sigma} \\ \hat{\alpha}\hat{e}_0 \exp[-\hat{\alpha}(i\hat{k} + \hat{k}^2)] & -1 - \hat{e}_0 \exp[-\hat{\alpha}(i\hat{k} + \hat{k}^2)] \end{bmatrix}. \quad (18)$$

While we have attempted to be maximally consistent in our scaling, it is worth noting that the IDE models have space re-parameterised in terms of the average downstream distance travelled by consumers per dispersal event, and not their lifetime advection.

The dependence of the spatial instability on model parameters is similar between the generalised emigration IDE (Fig. 4a,b) and the RDA model (Fig. 3c,d). The consumer emigration rate exhibits both ‘advection-like’ responses (via the $i\hat{k}$ term) and ‘diffusion-like’ responses (via the \hat{k}^2 term) seen in the RDA model. This is because the dispersal function $h(x, y)$ affects the consumer spatial distribution

in two ways. Like advection, it displaces the mean location of emigrants downstream, and like diffusion, it generates variance in dispersal distances.

We can make explicit the ‘advective’ and ‘diffusive’ components of dispersal in the IDE representation. By substituting $\varepsilon' = \beta = \delta$ and $\varepsilon = \hat{D} = 1$, we can see the analogy between eqs. (3) and (15) more clearly. Increasing the emigration sensitivity ε' destabilizes the system in a way that is similar to increasing the advection sensitivity β in the RDA model, despite also operating on the related \hat{k}^2 term as δ (Fig. 4a). In contrast, higher average emigration ε stabilizes high frequencies in a manner similar to increasing the contribution of diffusion to the average displacement distance (Fig. 4a,b). Thus, like diffusion in the RDA model, the effects of ε greatly lower \hat{k}_d and \hat{k}_{max} (Fig. 4a,b) but not \hat{k}_v over a large range of other parameter values.

The specified emigration IDE eq. (18) exhibits some special properties. The baseline emigration rate \hat{e}_0 and the sensitivity of emigration $\hat{\alpha}$ appear in both lower-row elements of eq. (18), meaning that changes in either parameter behaves in a way similar to *concurrently* altering de-stabilizing advection-like and stabilising diffusion-like processes in the RDA model. The dual, opposing effects of emigration parameters are quite apparent when changing the emigration sensitivity parameter $\hat{\alpha}$ (Fig. 4c). When small, increasing $\hat{\alpha}$ de-stabilizes the system and increases the range of unstable frequencies. When large, increasing $\hat{\alpha}$ re-stabilizes the system in a way similar to diffusion-like processes. The baseline emigration rate \hat{e}_0 de-stabilizes the system when increased which, interestingly, includes a noticeable expansion of de-stabilized low frequencies. This latter result arises from an increase in the average scale over which advection-like processes operate, allowing emigration sensitivity

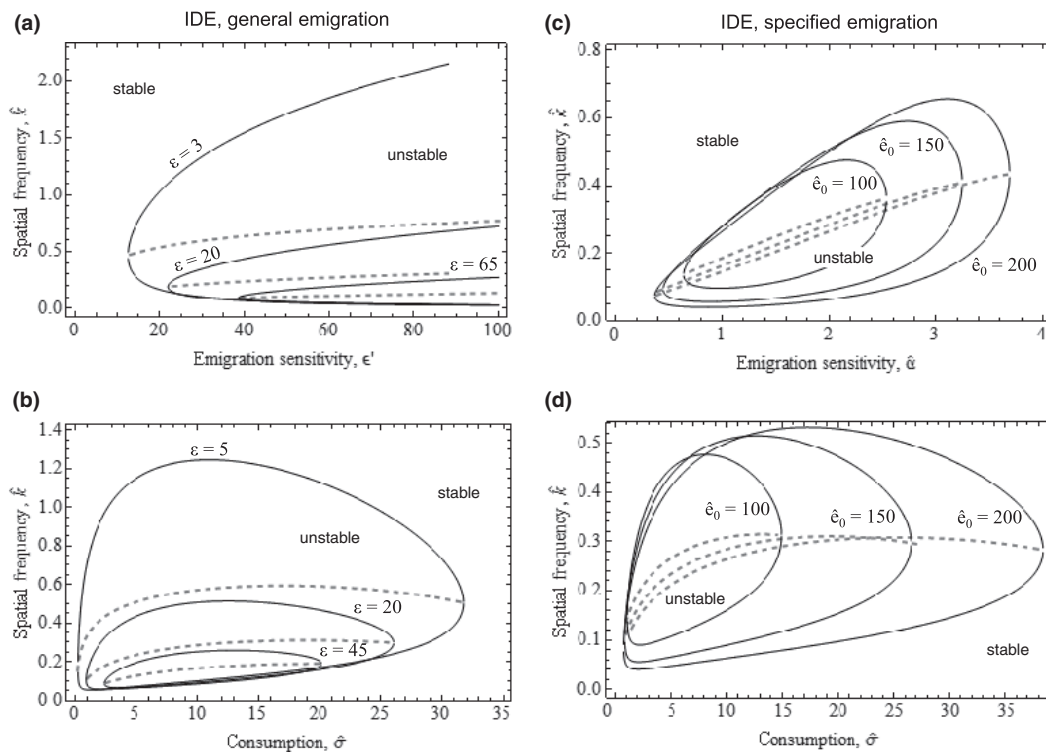


Figure 4 Effects of parameters on system stability in versions of the IDE model. Relationships between parameters and critical frequencies are as in Fig. 3. (a) General emigration model eq. (15), $\hat{\sigma} = 5$; (b) General emigration model eq. (15), $\varepsilon' = 40$; (c) Specified emigration model eq. (18), $\hat{\sigma} = 10$; (d) Specified emigration model eq. (18), $\beta = 2$.

(Fig. 4c) and consumption (Fig. 4d) to de-stabilize the system at both higher and lower frequencies over a range of values. This effect also means that the fastest growing frequency \hat{k}_{max} is relatively insensitive to changes in \hat{e}_0 (Fig. 4c,d).

DISCUSSION

Our goal was to examine the potential for spatial self-organisation in flowing water environments and other systems with biased transport. Using a model of an organism with downstream-biased dispersal, we explored how commonly observed traits of stream organisms (downstream drift, emigration dependence on resources, strong consumption control) influence the emergence of an instability that manifests as ‘waves’ of consumers and producers travelling downstream. We demonstrated that instability in our producer–consumer model does not require traditional ‘activator–inhibitor’ coupling through births and consumption. Thus, our model elucidates a less-restrictive mechanism for spatial pattern formation, involving consumer per capita emigration rates that vary with producer biomass, than is required in previous diffusion and flow-instability models.

Our instability also differs from other spatial pattern formation mechanisms that fall outside of traditional diffusive or FII ones. Because instability in our system requires the combination of consumption, producer-driven rates of consumer dispersal, and directional bias, it differs from other behaviourally driven spatial instability mechanisms that require movements that respond to conspecifics – rather than resources – to form (e.g. Lewis 1994; van de Koppel *et al.* 2008). Another large class of pattern formation mechanisms require the potential for unstable homogeneous-space dynamics as a necessary condition (e.g. Gurney & Veitch 2000 and references therein; Murray 2003; Malchow *et al.* 2008). These mechanisms are also not relevant here as equilibria in our system are always locally stable in both the absence of dispersal and to uniform global deviations from steady state (i.e. when $k = 0$) when dispersal is included. The local stability is due to the combination of open recruitment and a linear functional response describing consumption; we do anticipate that the addition of locally destabilizing recruitment or consumption terms (e.g. Nisbet *et al.* 1997) could interact with the mechanism we describe to yield quite rich dynamics.

Our results can be related to other, more general frameworks of endogenous spatial pattern formation. Rietkerk & Van de Koppel (2008) propose that a fundamental requirement for spatial instabilities is the co-occurrence of positive local reinforcement with long-range inhibition. In our system, positive local reinforcement occurs as a result of consumer per-capita emigration rates declining in concentrated areas of high producer biomass. Consumption creates areas of low producer biomass behind and ahead of producer concentrations. These areas in turn generate long-range inhibition when consumers quickly disperse through them as a result of high per-capita emigration rates coupled with directional dispersal.

Empirical implications

The strength of consumption, the maximum consumer emigration rate and the sensitivity of emigration to producer biomass are critical parameters in determining the existence and scale of instability. For the specified emigration IDE, it is possible to ‘guesstimate’ plausible ranges of parameters from literature sources. We use data from a meta-analysis of periphyton control by grazers across aquatic systems

to estimate consumption parameters (Hillebrand 2009) as well as from a set of open grazing experiments to estimate emigration parameters (*Baetis* mayflies: Kohler 1985; Forrester *et al.* 1999; Roll *et al.* (2005); multiple taxa: Diehl *et al.* 2008). Parameters are given in Table 1 and details of parameter estimation are provided in Online Supplement S3. Relating the parameters in Table 1 to the dimensionless parameters used in parameter studies requires dividing σC^* and e_0 by the consumer mortality rate m . Such rates likely vary widely from system to system depending on factors such as generation time, predation intensity, competition and disease. For example, Diehl *et al.* assumed $m = 0.01 \text{ day}^{-1}$ (average lifespan = 100 days) based on the overwintering life histories of their study organisms, whereas much higher mortality rates of 0.1 day^{-1} (average lifespan = 10 days) are probably not uncommon.

To examine the model behaviour under realistic parameter values, we pick a set of typical values from Table 1, $\sigma C^* = 0.23 \text{ day}^{-1}$, and $\alpha P^* = 2.0$, and set mortality to $m = 0.01 \text{ day}^{-1}$, which yields re-scaled consumption $\hat{\sigma} = 23$. From Fig. 4d, instability occurs when $100 < \hat{e}_0 < 150$; if we set this value to be $\hat{e}_0 = 135$, the selected value of αP^* yields $\bar{e}_G = 0.183 \text{ day}^{-1}$. This average per capita emigration rate is on the high end of our estimated range, as only four of seventeen species studied by Diehl *et al.* (2008) had values nearly equal or larger. However, reducing consumption to a less than typical value increases the range of emigration yielding instability. For example, setting $\hat{\sigma} = 5$ ($\sigma C^* = 0.05 \text{ day}^{-1}$) means the system becomes unstable when $\hat{e}_0 = 59$. This corresponds to $\bar{e}_G = 0.08 \text{ day}^{-1}$, which eight of seventeen species in Diehl *et al.* exceed. In contrast, setting mortality to $m = 0.1 \text{ day}^{-1}$ constrains our estimates of $\hat{e}_0 < 6$, essentially making instability impossible under the estimated ranges of other parameters. In total, these results suggest that stream systems where consumers have typical or lower than typical consumption rates, high movement potential and/or long lifespans are most likely to exhibit instability. Importantly, while our parameterisation exercise is admittedly crude, it does demonstrate that our described spatial instability is possible given realistic values.

As our instability is largely driven by dispersal away from areas of low resource biomass, the resulting spatial scale of variation is related to the scales over which transport processes operate. This result has generally been observed in other systems driven by flow-induced instabilities. For example, vegetation patterns in arid landscapes appear with periodicities in the order of tens of metres that are set by the downhill transport of water (Malchow *et al.* 2008). Aquatic ecosystems as diverse as tidal mudflats, coral reefs, ocean plankton and coastal wetlands show patterning from metres to kilometres

Table 1 Estimates for parameters or combinations of parameters from the specified IDE model eqs. (11) with consumption and emigration functions defined by eqs. (6) and (16) respectively

Parameter or combination estimated	Value	Study
σC^*	0–132 day^{-1} ; typical value of $\sim 0.23 \text{ day}^{-1}$	Hillebrand (2009)
e_0	$\sim 0.6 \text{ day}^{-1}$	Kohler (1985)
e_0	$\sim 0.03\text{--}0.09 \text{ day}^{-1}$	Forrester <i>et al.</i> (1999), Roll <i>et al.</i> (2005)
αP^*	$\sim 0.29\text{--}17$	Kohler (1985)
αP^*	$\sim 0.029\text{--}2.8$	Forrester <i>et al.</i> (1999), Roll <i>et al.</i> (2005)
$\bar{e}_G = e_0 \exp(-\alpha P^*)$	0.002–0.436 day^{-1}	Diehl <i>et al.</i> (2008)

depending on the scale over which flow transports nutrients or primary producers (Rietkerk & Van de Koppel 2008).

In our river model, instabilities are always much larger than the average length that consumers are transported in the drift during an emigration event (L_D). Lengths of drift events by aquatic macro-invertebrates have been observed to be anywhere from half a metre to 20 m or more, depending on the organism and flow velocities, with typical values being between 5 m and 10 m in the lower order streams (e.g. Elliott 1971). From our example above, typical values of $\hat{\epsilon}_0 = 135$, $\hat{\sigma} = 23$ and $\alpha P^* = 2.0$ yields a $\hat{k}_{max} \approx 0.3$ which translates into a spatial wavelength in the order of 100–200 m assuming typical drift distances, L_D , of around 10 m. This would place the scale over which instabilities will appear at the level of reaches or even whole rivers. Large-scale variation in consumers and resources could therefore be quite divergent from local dynamics, making our results consistent with the argument by Woodward & Hildrew (2002) and others that ‘intergenerational’ components of food webs will be most apparent, and should be examined, at the landscape scale. However, we caution that nutrients (Newbold 1992), primary producers (Simpson *et al.* 2008) and other organisms are also subjected to redistribution via directed dispersal, which could lead to additional instabilities at different scales. Understanding transport processes of these components is key to discerning the effects of how locally observed interactions manifest at other scales.

Spatial patterns emerging from our instability may be difficult to discern empirically unless they are specifically sought after over scales larger than transport processes operate. A data series of longitudinal samples, for example, might show a power spectrum with a peak near k_{max} that should generally be larger than other periodic river features (e.g. riffles and pools). In addition, k_{max} could be predicted using small scale parameterisation experiments. Although coarser than our recommendation, recent multi-scale studies have found stronger negative correlations between consumers and resources – and resource suppression generally – at the riffle to reach scale compared with microhabitat or laboratory scales (Feminella & Hawkins 1995; Wellnitz *et al.* 2001; Taylor *et al.* 2002; Doi & Katano 2008). Large-scale (>2 km) suppression of resource biomass was also observed to strengthen as caddisfly consumers invaded downstream-stream reaches in a wave-like fashion following initial upstream colonisation (Katano *et al.* 2007) similar to dynamics observed in our model. This wave traversed downstream reaches over the course of a season. Given that wave speeds in our model are proportional to the average consumer-lifetime, the observations in Katano *et al.* (2007) are roughly consistent with temporal and spatial dynamics predicted by our parameter estimates, though, of course, an invasion wave need not be driven by the same mechanisms that excite waves in an established population. Suppression of filamentous microalgae by the caddisflies coincided with increases in small diatoms, implying that travelling wave instabilities could create refuges from competition or have other cascading community-wide effects that vary spatially and temporally.

We have shown that instability can generate spatial patterns within given realistic parameter values. Using a more restricted variant of eq. (12), we have also shown that strong transient spatial patterns can occur even when equilibria are stable (Anderson *et al.* 2008). This suggests that endogenous spatial pattern formation could occur over a wider range of parameters than predicted by our stability analysis. In the transition to instability, we found that transient dynamics exhibit a scale-dependence similar to the fully unstable system. In other words, a stable consumer–producer system may exhibit transient

waves at spatial scales similar to those predicted in unstable parameter regions. Given the highly temporally variable nature of many flowing systems, it could be that transient patterns – growth of deviations near steady state in stable and unstable systems – are more empirically discernible than the persistent patterns that take many time steps to finalise (Supplement S2). Regardless, both persistent and transient spatial patterning add to the growing bestiary of spatial dynamics observed in recent theory of flowing environments (e.g. Speirs & Gurney 2001; Levine 2003; Lutscher *et al.* 2005, 2007; Pachepsky *et al.* 2005; Anderson *et al.* 2006; Malchow *et al.* 2008), which provides a powerful toolbox for unravelling the causes and consequences of spatial variation.

ACKNOWLEDGEMENTS

The authors thank Fred Adler, Thomas Hillen, Mark Lewis, Frithjof Lutscher and three anonymous referees for helpful discussions and comments on earlier versions of this manuscript. Funding was provided by NSF award DEB-0717259 to RMN, by Alberta Ingenuity and Honorary Killam Fellowships to FMH, and by the University of California, Riverside to KEA.

AUTHORSHIP

KEA, FMH, and RMN contributed to model analysis. KEA wrote the initial draft of the manuscript, and KEA, FMH and RMN contributed substantially to revisions.

REFERENCES

- Anderson, K.E., Nisbet, R.M. & Diehl, S. (2006). Spatial scaling of consumer–resource interactions in advection-dominated systems. *Am. Nat.*, 168, 358–372.
- Anderson, K.E., Nisbet, R.M. & McCauley, E. (2008). Transient responses to spatial perturbations in advective systems. *B. Math. Biol.*, 70, 1480–1502.
- Byers, J.E. & Pringle, J.M. (2006). Going against the flow: retention, range limits and invasions in advective environments. *Mar. Ecol. Prog. Ser.*, 313, 27–41.
- Cooper, S.D., Diehl, S., Kratz, K. & Sarnelle, O. (1998). Implications of scale for patterns and processes in stream ecology. *Aust. J. Ecol.*, 23, 27–40.
- Diehl, S., Cooper, S.D., Kratz, K.W., Nisbet, R.M., Roll, S.K., Wiseman, S.W. *et al.* (2000). Effects of multiple, predator-induced behaviors on short-term producer–grazer dynamics in open systems. *Am. Nat.*, 156, 293–313.
- Diehl, S., Anderson, K.E. & Nisbet, R.M. (2008). Population responses of drifting stream invertebrates to spatial environmental variability: new theoretical developments. In: *Aquatic Insects: Challenges to Populations* (eds Lancaster, J. & Briers, R.A.). CABI Publishing, Wallingford, UK, pp. 158–183.
- Doi, H. & Katano, I. (2008). Distribution patterns of stream grazers and relationships between grazers and periphyton at multiple spatial scales. *J. N. Am. Benthol. Soc.*, 27, 295–303.
- Elliott, J.M. (1971). The distances travelled by drifting invertebrates in a Lake District stream. *Oecologia*, 6, 350–379.
- Englund, G. & Hambäck, P.A. (2004). Scale-dependence of movement rates in stream invertebrates. *Oikos*, 105, 31.
- Englund, G., Cooper, S.D. & Sarnelle, O. (2001). Application of a model of scale dependence to quantify scale domains in open predation experiments. *Oikos*, 92, 501–514.
- Feminella, J.W. & Hawkins, C.P. (1995). Interactions between stream herbivores and periphyton: a quantitative analysis of past experiments. *J. N. Am. Benthol. Soc.*, 14, 465–509.
- Fonseca, D.M. & Hart, D.D. (1996). Density-dependent dispersal of black fly neonates is mediated by flow. *Oikos*, 75, 49–58.
- Forrester, G.E., Dudley, T.L. & Grimm, N.B. (1999). Trophic interactions in open systems: effects of predators and nutrients on stream food chains. *Limnol. Oceanogr.*, 44, 1187–1197.

- Gurney, W.S.C. & Veitch, A.R. (2000). Self-organization, scale and stability in a spatial predator-prey interaction. *Bull. Math. Biol.*, 62, 61–86.
- Hillebrand, H. (2009). Meta-analysis of grazer control of periphyton biomass across aquatic ecosystems. *J. Phycol.*, 45, 798–806.
- Katano, I., Doi, H., Houki, A., Isobe, Y. & Oishi, T. (2007). Changes in periphyton abundance and community structure with the dispersal of a caddisfly grazer, *Micrasema quadriloba*. *Limnology*, 8, 219–226.
- Kohler, S.L. (1985). Identification of stream drift mechanisms: an experimental and observational approach. *Ecology*, 66, 1749–1761.
- van de Koppel, J., Rietkerk, M., Dankers, N. & Herman, P.M.J. (2005). Scale-dependent feedback and regular spatial patterns in young mussel beds. *Am. Nat.*, 165, E66–E77.
- van de Koppel, J., Gascoigne, J.C., Theraulaz, G., Rietkerk, M., Mooij, W.M. & Herman, P.M.J. (2008). Experimental evidence for spatial self-organization and its emergent effects in mussel bed ecosystems. *Science*, 322, 739–742.
- Levine, J.M. (2003). A patch modeling approach to the community-level consequences of directional dispersal. *Ecology*, 84, 1215–1224.
- Lewis, M.A. (1994). Spatial coupling of plant and herbivore dynamics – the contribution of herbivore dispersal to transient and persistent waves of damage. *Theor. Popul. Biol.*, 45, 277–312.
- Lutscher, F., Pachepsky, E. & Lewis, M.A. (2005). The effect of dispersal patterns on stream populations. *SIAM Rev.*, 47, 749–772.
- Lutscher, F., McCauley, E. & Lewis, M.A. (2007). Spatial patterns and coexistence mechanisms in systems with unidirectional flow. *Theor. Popul. Biol.*, 71, 267–277.
- Malchow, H., Petrovskii, S.V. & Venturino, E. (2008). *Spatiotemporal Patterns in Ecology and Epidemiology: Theory, Models, and Simulations*. Mathematical and Computational Biology Series. Chapman & Hall/CRC Press, Boca Raton.
- Murray, J.D. (2003). *Mathematical Biology*, 3rd edn. Springer, New York.
- Newbold, J.D. (1992). Cycles and spirals of nutrients 1. Hydrological and ecological principles. In: *The Rivers Handbook* (eds Calow, P. & Petts, G.). Blackwell Scientific, Oxford, pp. 379–408.
- Nisbet, R.M., Diehl, S., Wilson, W.G., Cooper, S.D., Donalson, D.D. & Kratz, K. (1997). Primary-productivity gradients and short-term population dynamics in open systems. *Ecol. Monogr.*, 67, 535–553.
- Pachepsky, E., Lutscher, F., Nisbet, R.M. & Lewis, M.A. (2005). Persistence, spread and the drift paradox. *Theor. Popul. Biol.*, 67, 61.
- Palmer, M.A., Allan, J.D. & Butman, C.A. (1996). Dispersal as a regional process affecting the local dynamics of marine and stream benthic invertebrates. *Trends Ecol. Evol.*, 11, 322–326.
- Rader, R.B. (1997). A functional classification of drift: traits that influence invertebrate availability to salmonids. *Can. J. Fish. Aquat. Sci.*, 54, 1211–1234.
- Rietkerk, M. & Van de Koppel, J. (2008). Regular pattern formation in real ecosystems. *Trends Ecol. Evol.*, 23, 169–175.
- Roll, S.K., Diehl, S. & Cooper, S.D. (2005). Effects of grazer immigration and nutrient enrichment on an open algae-grazer system. *Oikos*, 108, 386–400.
- Rovinsky, A.B. & Menzinger, M. (1992). Chemical-instability induced by a differential flow. *Phys. Rev. Lett.*, 69, 1193–1196.
- Segel, L.A. & Jackson, J.L. (1972). Dissipative structure: an explanation and an ecological example. *J. Theor. Biol.*, 37, 545–559.
- Sherratt, J.A. (2005). An analysis of vegetation stripe formation in semi-arid landscapes. *J. Math. Biol.*, 51, 183–197.
- Simpson, K., McCauley, E. & Nelson, W.A. (2008). Spatial heterogeneity and rates of spread in experimental streams. *Oikos*, 117, 1491–1499.
- Speirs, D.C. & Gurney, W.S.C. (2001). Population persistence in rivers and estuaries. *Ecology*, 82, 1219–1237.
- Taylor, B.W., McIntosh, A.R. & Peckarsky, B.L. (2002). Reach-scale manipulations show invertebrate grazers depress algal resources in streams. *Limnol. Oceanogr.*, 47, 893–899.
- Townsend, C.R. (1989). The patch dynamics concept of stream community ecology. *J. N. Am. Benthol. Soc.*, 8, 36–50.
- Vannote, R.L., Minshall, G.W., Cummins, K.W., Sedell, J.R. & Cushing, C.E. (1980). The river continuum concept. *Can. J. Fish. Aquat. Sci.*, 37, 130–137.
- Waters, T.F. (1972). The drift of stream insects. *Annu. Rev. Entomol.*, 17, 253–272.
- Wellnitz, T.A., Poff, N.L., Cosyleon, G. & Steury, B. (2001). Current velocity and spatial scale as determinants of the distribution and abundance of two rheophilic herbivorous insects. *Landsc. Ecol.*, 16, 111–120.
- Williams, D.D. & Williams, N.E. (1993). The upstream/downstream movement paradox of lotic invertebrates: quantitative evidence from a Welsh mountain stream. *Freshwater Biol.*, 30, 199–218.
- Winterbottom, J., Orton, S. & Hildrew, A. (1997). Field experiments on the mobility of benthic invertebrates in a southern English stream. *Freshwater Biol.*, 38, 37–47.
- Woodward, G. & Hildrew, A.G. (2002). Food web structure in riverine landscapes. *Freshwater Biol.*, 47, 777–798.

SUPPORTING INFORMATION

Additional Supporting Information may be downloaded via the online version of this article at Wiley Online Library (www.ecologyletters.com).

As a service to our authors and readers, this journal provides supporting information supplied by the authors. Such materials are peer-reviewed and may be re-organised for online delivery, but are not copy edited or typeset. Technical support issues arising from supporting information (other than missing files) should be addressed to the authors.

Editor, Frederick Adler

Manuscript received 6 June 2011

First Decision made 8 July 2011

Second Decision made 13 October 2011

Manuscript accepted 28 November 2011